$Nd_2Sn_2O_7$: An all-in–all-out pyrochlore magnet with no divergence-free field and anomalously slow paramagnetic spin dynamics

A. Bertin,[1,2] P. Dalmas de Réotier,[1,2,*] B. Fåk,[1,2] C. Marin,[1,2] A. Yaouanc,[1,2] A. Forget,[3] D. Sheptyakov,[4] B. Frick,[5] C. Ritter,[5] A. Amato,[6] C. Baines,[6] and P. J. C. King[7]

[1]*Université Grenoble Alpes, INAC-SPSMS, F-38000 Grenoble, France*

[2]*CEA, INAC-SPSMS, F-38000 Grenoble, France*

[3]*Institut Rayonnement Matière de Saclay, SPEC, CEA, F-91191 Gif-sur-Yvette, France*

[4]*Laboratory for Neutron Scattering and Imaging, Paul Scherrer Institute, CH-5232 Villigen-PSI, Switzerland*

[5]*Institut Laue-Langevin, Boite Postale 156X, F-38042 Grenoble Cedex 9, France*

[6]*Laboratory for Muon-Spin Spectroscopy, Paul Scherrer Institute, CH-5232 Villigen-PSI, Switzerland*

[7]*ISIS Facility, Rutherford Appleton Laboratory, Chilton, Didcot OX11 0QX, United Kingdom*

(Received 17 July 2014; revised manuscript received 10 September 2015; published 26 October 2015)

We report measurements performed on a polycrystalline sample of the pyrochlore compound $Nd_2Sn_2O_7$. It undergoes a second order magnetic phase transition at $T_c \approx 0.91$ K to a noncoplanar all-in–all-out magnetic structure of the Nd^{3+} magnetic moments. The thermal behavior of the low temperature specific heat fingerprints excitations with linear dispersion in a three-dimensional lattice. The temperature independent spin-lattice relaxation rate measured below T_c and the anomalously slow paramagnetic spin dynamics detected up to $\approx 30T_c$ are suggested to be due to magnetic short-range correlations in unidimensional spin clusters, i.e., spin loops. The observation of a spontaneous field in muon spin relaxation measurements is associated with the absence of a divergence-free field for the ground state of an all-in–all-out pyrochlore magnet as predicted recently.

DOI: 10.1103/PhysRevB.92.144423 PACS number(s): 75.25.−j, 75.40.−s, 76.75.+i, 78.70.Nx

I. INTRODUCTION

The pyrochlore insulator compounds of generic chemical formula $R_2M_2O_7$, where R is a rare earth ion and M a nonmagnetic element, are a fertile playground for the discovery of exotic magnetic properties [1]. The most enigmatic results were found for their spin dynamics. At least two signatures of them have been recognized.

First, persistent spin dynamics as inferred from a finite spin-lattice relaxation rate measured at low temperature by the zero-field muon spin relaxation (μSR) technique is a ubiquitous physical property of the ground state, no matter its magnetic nature. Low-energy unidimensional excitations have recently been argued to be at its origin [2]. They could be supported by spin loops, i.e., peculiar short-range correlations [3,4].

In μSR measurements, the signature of a transition to a magnetically ordered state is the observation of muon spin precession corresponding to a spontaneous field at the muon site. While in neutron scattering experiments at low temperatures, $Er_2Ti_2O_7$, $Tb_2Sn_2O_7$, and $Yb_2Sn_2O_7$ display magnetic Bragg reflections characterized by a propagation wave vector $\mathbf{k} = (0,0,0)$ [5–7], no spontaneous precession is observed in μSR measurements [7–9]. This is the second unexpected result. In contrast, spontaneous fields have been reported for $Gd_2Ti_2O_7$ [10]. However, this is a system with a complex magnetic structure [11]. More interesting, $Gd_2Sn_2O_7$ displays a $\mathbf{k} = (0,0,0)$ structure [12] and spontaneous fields [13,14]. A fraction of the μSR signal is missing in the ordered state, probably because of the large field distribution at the magnetic sites corresponding to this fraction. In this context the characterization of a compound with a $\mathbf{k} = (0,0,0)$ magnetic order together with a spontaneous field with no missing fraction would provide further insight.

Here we report a study of the cubic pyrochlore stannate $Nd_2Sn_2O_7$ [15,16], with specific heat, magnetization, neutron scattering, and μSR measurements. It exhibits a magnetic phase transition at $T_c \approx 0.91$ K to a so-called all-in–all-out magnetic structure with a $\mathbf{k} = (0,0,0)$ propagation wave vector. A μSR spontaneous field is observed, consistent with the lack of the divergence-free part of the Helmholtz decomposition of the magnetic-moment field for such a magnetic structure [17]. In this frame, the long-range order is associated with the divergence-full component of the field. Persistent spin dynamics below T_c and an anomalously slow paramagnetic spin dynamics up to $\approx 30\ T_c$ are detected. They are suggested to be due to unidimensional spin loops.

We first establish the basic physical characteristics of the compound from bulk measurements and neutron scattering experiments. Further microscopic information on the static and dynamical properties of the system is obtained from inelastic neutron scattering and μSR experiments. A discussion of the results completes this report.

II. BULK MEASUREMENTS

A single-phase powder sample of $Nd_2Sn_2O_7$ was prepared by heating the constituent oxides up to 1400°C with four intermediate grindings. The heat capacity C_p recorded with a Physical Property Measurement System (Quantum Design Inc.) is presented in Fig. 1(a). It matches previous results [18] in the overlapping temperature range. A λ-type peak consistent with a second-order phase transition is observed at $T_c \approx 0.91$ K, i.e., the temperature of a peak in magnetic susceptibility data [19]. No broad hump above T_c is present, unlike in some geometrically frustrated magnets, where it is interpreted

*Electronic address: pierre.dalmas-de-reotier@cea.fr

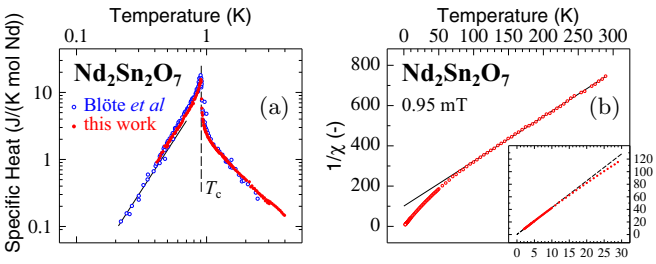

FIG. 1. (Color online) Bulk measurements for a $Nd_2Sn_2O_7$ powder sample. (a) Specific heat versus temperature. Our results are compared with those in Ref. [18]. (b) Temperature dependence of the inverse magnetic susceptibility $1/\chi$ expressed in SI units and measured in a field of 0.95 mT. Inset: Low-temperature data. The sample used for this measurement was a thin pellet and the field was applied in its plane so as to minimize demagnetization field effects. In both panels, solid lines are results of fits as explained in the text.

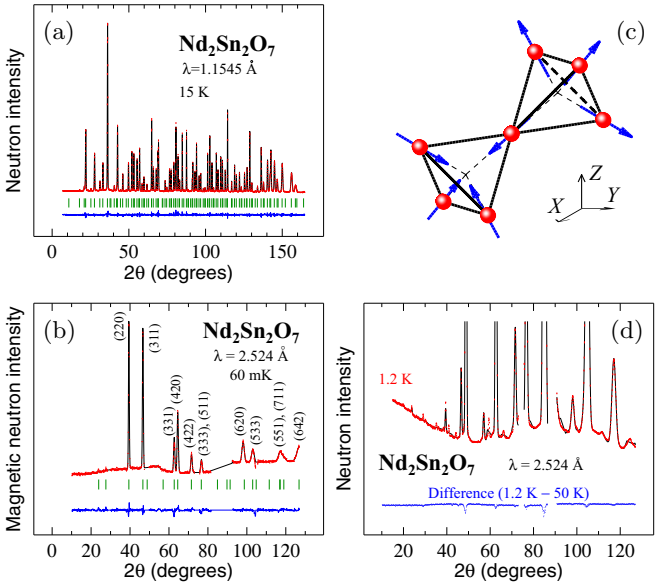

FIG. 2. (Color online) Neutron diffraction results for a powder sample of $Nd_2Sn_2O_7$. (a) Nuclear pattern at $T = 15$ K. (b) Magnetic diagram given by the difference between 60 mK and 1.2 K data sets. Experimental points near $2\theta = 74.4^\circ$ and 88.5° are not shown because they are strongly influenced by neutrons scattered from the copper container. The observed magnetic reflections are labeled with Miller indices. (a, b) Solid lines result from Rietveld analyses. Solid lines at the bottom give the difference between fits and data. Vertical markers indicate the positions of Bragg peaks. (c) The corresponding magnetic structure. Spheres represent Nd^{3+} ions, and arrows their magnetic moments oriented along the local trigonal $\langle 111 \rangle$ axes of the cubic crystal structure. Two corner-sharing tetrahedra are shown, one with the magnetic moments pointing inwards and another, adjacent tetrahedron with moments pointing outwards. (d) Diffractogram recorded at 1.2 K and difference from the data set recorded at 50 K. No diffuse scattering intensity is observed at the approach of the magnetic transition. Note that for the sake of clarity, the most intense Bragg peaks present at 1.2 K have been truncated.

as a signature of short-range correlations [20]. The law $C_p = \mathcal{B}T^3$ accounts for the data at low temperatures [Fig. 1(a)]. This temperature dependence is expected for excitations with a linear dispersion relation in a three-dimensional system. It sets a higher bound for any gap in the excitation spectrum at $\approx$0.1 meV. From the value $\mathcal{B} = 11.0\,(7)$ J K^{-4} mol^{-1} obtained from data measured below 0.45 K, we infer an excitation velocity $v_{ex} = 55\,(1)$ m s^{-1} in line with the $Er_2Ti_2O_7$ result [21].

In Fig. 1(b) is displayed the inverse of the static susceptibility $1/\chi$. In the temperature range $150 \leqslant T \leqslant 290$ K χ follows a Curie-Weiss law, with a Curie-Weiss temperature $\theta_{CW} = -46.3\,(1.9)$ K and a paramagnetic moment $m_{pm} = 3.57(4)\mu_B$, comparable with the value $m_{pm} = 3.62\mu_B$ for a free Nd^{3+} ion. As shown in the inset, assuming χ to follow a Curie-Weiss law for $5 \leqslant T \leqslant 15$ K we get $\theta_{CW} = -0.32$ (1) K and $m_{pm} = 2.63\,(3)\mu_B$, in agreement with Ref. [22]. The negative θ_{CW} indicates net antiferromagnetic exchange interactions. As the first excited crystal-field doublet is located at $\approx$26 meV above the Kramers doublet of the Nd^{3+} ground state [23], an effective spin $S' = 1/2$ model is justified for the ion description at low temperatures.

III. NEUTRON DIFFRACTION RESULTS

$Nd_2Sn_2O_7$ crystallizes in the $Fd\bar{3}m$ space group. We studied the crystal structure of our sample using the diffractometers D2B at Institut Laue Langevin (ILL) and HRPT of the SINQ neutron source at the Paul Scherrer Institute (PSI), respectively, at room temperature and 15 K. Figure 2(a) displays the HRPT data analyzed with the FullProf suite [24]. The lattice parameter is $a_{lat} = 10.5586\,(6)$ Å and the parameter for the oxygen position is $x = 0.33259\,(3)$ at 15 K; see Fig. 2(a) for the diffraction pattern. For comparison, the corresponding room temperature values obtained in our D2B measurements are $a_{lat} = 10.568\,(3)$ Å and $x = 0.33250\,(8)$, in agreement with the literature [16]. Our Rietveld refinement revealed a slight stuffing and oxygen deficiency: with the notation $Nd_{2+y}Sn_{2-y}O_{7+\delta}$ we got $y = 0.013\,(7)$ and $\delta = -0.006\,(3)$ [23].

Magnetic neutron diffraction measurements were performed with the D1B diffractometer at ILL. In Fig. 2(b) a *magnetic* diffraction diagram at 60 mK is presented. The Bragg reflections imply a long-range order of the Nd^{3+} magnetic moments to be established. The reflections occurring only at the nuclear Bragg peak positions, the magnetic propagation vector of the structure is $\mathbf{k} = (0,0,0)$. The absence of magnetic intensity at positions (111), (200), and (400) is consistent with the noncoplanar all-in–all-out moment arrangement shown in Fig. 2(c) [23]. It is confirmed by an analysis with FullProf. The spontaneous magnetic moment is $m_{sp}(T \to 0) \simeq m_{sp}(T = 0.06\text{ K}) = 1.708(3)\mu_B$. The all-in–all-out magnetic structure was first reported for FeF_3 [25] and subsequently observed for the Nd^{3+} moments and proposed for the Ir moments of $Nd_2Ir_2O_7$ [26] and for the Os moments of $Cd_2Os_2O_7$ [27,28]. It was also deduced from an analysis of resonant x-ray diffraction data obtained for $Eu_2Ir_2O_7$ [29]. This structure should not give rise to a structural distortion [29], consistent with the second-order nature of the magnetic phase transition. We, finally, mention that no diffuse scattering which would signal the onset of short-range magnetic correlations is observed when

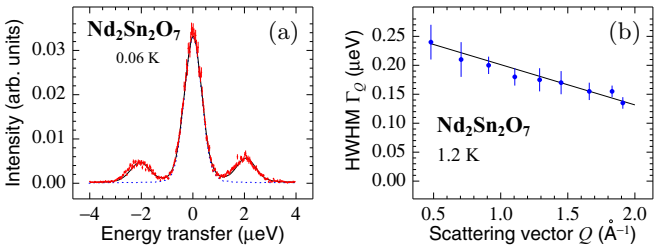

FIG. 3. (Color online) Inelastic neutron scattering results for a $Nd_2Sn_2O_7$ powder sample. (a) Wave-vector integrated backscattering spectrum at 0.06 K. The instrument resolution determined from an independent measurement on vanadium is shown by the dotted line. (b) Wave-vector dependence of the quasielastic half-width at half-maximum (HWHM) Γ_Q of the magnetic scattering in the paramagnetic phase at 1.2 K. In both panels, solid lines are results of fits as explained in the text.

approaching the magnetic transition from the paramagnetic phase, unlike in, e.g., $Tb_2Sn_2O_7$ [6] [see Fig. 2(d)].

IV. INELASTIC NEUTRON SCATTERING RESULTS

For an independent estimate of m_{sp} and to gather information on the spin dynamics up to the 10^{-9} s range, we performed neutron backscattering measurements at the IN16 backscattering spectrometer at ILL. The inelastic scattering intensity measured at $\approx\pm 2\ \mu$eV [Fig. 3(a)] in the magnetically ordered phase corresponds to transitions among the nuclear spin levels whose degeneracy is lifted by the hyperfine field [30]. This is an incoherent scattering process. Among the Nd isotopes the contribution of ^{143}Nd overwhelmingly dominates due to its large incoherent scattering cross section. The splitting $\hbar\omega_Z = 2.027(7)\ \mu$eV measured at 0.06 K corresponds to $m_{sp} = \hbar\omega_Z/\mathcal{A}^{143}_{hyp} = 1.68(3)\mu_B$ using the hyperfine constant $\mathcal{A}^{143}_{hyp} = 20.9(3)$ mT [31]. The incoherent nature of the scattering process implies that each nucleus is probed additively; i.e., there are no interference effects as in diffraction. Hence, backscattering provides a *local probe determination* of m_{sp}. Diffraction, which measures a volume average [32], and backscattering data giving consistent results, no phase segregation occurs in our sample.

Information about spin dynamics is obtained from backscattering data recorded at 1.2 K, i.e., above T_c. Besides the nuclear incoherent scattering, a signal of electronic origin is observed which is broader than the experimental resolution. Fitting this signal using a Lorentzian function we deduce the quasielastic half-width at half-maximum Γ_Q. We find it to be weakly Q dependent with a linear wave-vector dependence $\Gamma_Q = \Gamma_0 + a_Q Q$, where $\Gamma_0 = 0.271(9)\ \mu$eV and $a_Q = -0.070(2)\ \mu$eV Å [see Fig. 3(b)]. While more data would be needed to discuss this Q dependence, we notice the linewidth to be in the range $\Gamma_{BS} \simeq 0.2\ \mu$eV, which corresponds to a fluctuation time $\tau_{BS} = \hbar/\Gamma_{BS} = 3\times 10^{-9}$ s. This is relatively slow for a temperature outside the critical regime. We would have expected a time of order $\hbar/(k_B|\theta_{CW}|) = 2.4(1)\times 10^{-11}$ s, where we take θ_{CW} derived from the $\chi(T)$ fit at low temperature. Even slower paramagnetic fluctuations are revealed by the μSR study discussed below.

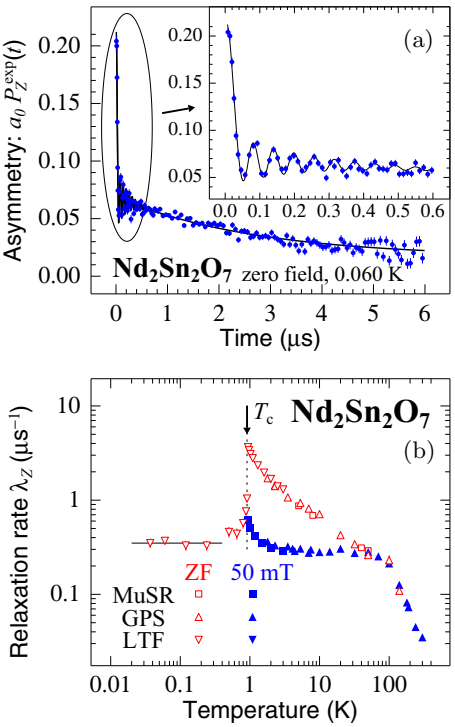

FIG. 4. (Color online) μSR results. (a) An asymmetry spectrum recorded deep in the ordered state (LTF spectrometer). The solid line results from a phenomenological fit. Inset: The short-time part of the spectrum. (b) Temperature dependence of the spin-lattice relaxation rate λ_Z in zero field (open symbols) and for $B_{ext} = 50$ mT (filled symbols). Data were recorded at different spectrometers as indicated. The T_c value is shown as the dotted line and the solid line emphasizes the temperature-independent zero-field λ_Z at low temperatures.

V. μSR RESULTS

Further information was obtained from μSR measurements performed at the MuSR spectrometer of the ISIS pulsed muon source (Rutherford Appleton Laboratory, UK) and at the GPS and LTF spectrometers of the Swiss Muon Source at PSI. All data were recorded with longitudinal geometry, either in zero field or under a longitudinal field. These different variants of the technique probe the magnetic properties of the system on a time scale ranging from approximately 10^{-5} to 10^{-12} s. A μSR asymmetry spectrum recorded below T_c is shown in Fig. 4(a). The displayed quantity is $a_0 P_Z^{exp}(t)$, where a_0 is an experimental parameter and $P_Z^{exp}(t)$ is the muon polarization function, which reflects the physics of the compound under study [33]. We observe a sharp drop in the asymmetry at short times, followed by a slow exponential decay of the tail. Its decay rate is a measure of the spin-lattice relaxation rate λ_Z. The early-time part of the spectrum is detailed in the inset. A spontaneous (i.e., in the absence of an external field) muon spin precession is detected. This is so up to $T \leqslant 0.65\ \text{K} \approx 0.7T_c$. It reflects the long-range magnetic order. Although a spontaneous muon spin precession is expected and often observed in the ordered phase of magnets, including exotic magnets [34], it is not present, as mentioned earlier, for $Tb_2Sn_2O_7$ [9,35], $Er_2Ti_2O_7$ [8,36], or $Yb_2Sn_2O_7$ [7,37] or for $CdHo_2S_4$ [2]. This has been attributed to the dynamical

nature of the field at the muon site [9]. Above $\approx 0.7T_c$, the muon spin precession is not resolved: this is probably due to a broadening of the field distribution at the muon site and dynamical effects. In the whole temperature range below T_c the spin-lattice relaxation channel is easily observed. The function $a_0 P_Z^{\rm exp}(t) = a_s P_Z(t) + a_{\rm bg}$ was fitted to all the spectra. The first term is associated with muons probing the sample and the second, time-independent component accounts for muons implanted in the sample surroundings. Above T_c a stretched exponential function, $P_Z(t) = \exp[-(\lambda_Z t)^{\beta_{\rm se}}]$, with the exponent $0.7 \leqslant \beta_{\rm se} \leqslant 1$, provides a good description of the spectra. Such a spectral shape is consistent with a distribution of relaxation channels and is often observed in frustrated magnets.

In Fig. 4(b), $\lambda_Z(T)$ deduced from zero-field and 50-mT measurements is plotted. These data are remarkable in many respects. In zero field $\lambda_Z(T)$ displays a pronounced maximum at T_c. This reflects the slowing-down of the critical fluctuations at the approach of a second-order magnetic phase transition. At $T \ll T_c$ we would expect λ_Z to vanish [33,38–40]. The plateau that is instead observed, the signature of the so-called persistent spin dynamics, has been ascribed to unidimensional excitations [2] which could be present in lattices of corner-sharing triangles or tetrahedra. The λ_Z thermal behavior above its inflection point at ≈ 100 K is driven by an Orbach local relaxation mechanism [20,33]. At lower temperatures, but still in the paramagnetic regime, correlations come into play. However, their characteristics are not as expected for a conventional paramagnetic phase. This key new result is dramatically revealed by the strong dependence of λ_Z on $B_{\rm ext}$. Quite unexpectedly, its influence extends up to about 30 K, i.e., $\approx 30T_c$. Because of this strong $B_{\rm ext}$ dependence of λ_Z at low field and the plateau observed for $\lambda_Z(T)$ under 50 mT for $2 < T < 100$ K, using the model due to Redfield [41] we infer the presence of spin fluctuations with a correlation time $\tau_{\mu\rm SR}$ in the 100-ns range. Hence, the zero-field fluctuations probed by μSR are characterized by a $\tau_{\mu\rm SR}$ much larger than the time estimated from the quasielastic neutron scattering data, i.e., $\tau_{\rm BS}$. $Nd_2Sn_2O_7$ is not a unique example of this feature [42]. In fact, a wide range of correlation times extending to anomalously long times seems to be a signature of geometrically frustrated magnetic materials [21,36,43–48].

VI. DISCUSSION AND CONCLUSIONS

We now discuss the prominent experimental results obtained from our experimental study, namely, (i) the all-in–all-out type of magnetic structure found for $Nd_2Sn_2O_7$, (ii) the observation of a spontaneous field in μSR measurements, while this field is not detected in some other magnetically ordered pyrochlores, and (iii) the anomalously slow dynamics in the paramagnetic phase.

The all-in–all-out magnetic structure has been predicted for antiferromagnetically coupled Ising spins [49]. However, the T^3 temperature dependence of the specific heat implies that magnon-like excitations are present and therefore the spins cannot be entirely Ising-like. A recent computation using a gauge mean-field approximation and incorporating spin-exchange terms other than the Ising term has appeared [50]. It predicts the all-in–all-out phase for a range of exchange parameters. Unfortunately this result cannot be tested since no formulas for the velocity $v_{\rm ex}$ or the static susceptibility χ in terms of exchange parameters have been given.

Recently the concept of fragmentation for Ising anisotropy pyrochlore compounds was introduced [17]. The field associated with the magnetic moments of an isolated tetrahedron is proposed to split into divergence-full and divergence-free parts. Within this model a long-range order is modeled by the first part of the Helmholtz decomposition. The second part corresponds to a fluid of monopoles. Since the divergence-free field does not exist for the ground state of the all-in–all-out magnetic structure, there is no reason for the spontaneous field to flip [9], and therefore its detection for $Nd_2Sn_2O_7$ is naturally explained. We note that the low-temperature moment is not collinear with the local threefold axis for $Tb_2Sn_2O_7$, $Yb_2Sn_2O_7$, and $Yb_2Ti_2O_7$. Hence the fragmentation model in its present status is not applicable to these three compounds. Note that the physics of $Tb_2Sn_2O_7$ is, in any case, complicated because Tb^{3+} is a non-Kramers doublet and therefore the lattice is subject to crystallographic distortions.

Slow paramagnetic dynamics might be a general property of magnetic pyrochlore compounds. It was uncovered early on for $Tb_2Ti_2O_7$ [43]. It has recently been characterized in $Yb_2Ti_2O_7$ and $Yb_2Sn_2O_7$ [47]. As to its origin, emergent unidimensional spin clusters—spin loops—i.e., peculiar molecular spin structures, are a natural candidate. Excitations supported by these structures were recently suggested to drive persistent spin dynamics for $T \ll T_c$ as measured by λ_Z [2]. The interactions between quasiparticles above T_c may renormalize them, which would lead to the observed temperature dependence of λ_Z. Spins involved in these structures are expected to display short-range correlation effects and their dynamics should be relatively slow in comparison to magnetically isolated spins. These structures have rarely been discussed theoretically [3,4,51]. They are a natural occurrence in pyrochlore and kagome lattices.

While spin dynamics has been consistently observed in numerous studies of pyrochlore systems, the present work suggests that it signals phenomena of quite different origins. The temperature-independent μSR rate when $T \to 0$ and the anomalously slow dynamics revealed here are attributed to correlated spin loops. The absence of a spontaneous field would result from the divergence-free part of the magnetization field in compounds with components of their magnetic moments along local threefold axes.

For further progress, the published fragmentation model, which only considers classical Ising spins [17], should be generalized to quantum spins with components perpendicular to the local threefold axis [52]. The generic nature of the unidimensional excitations should be addressed. On the experimental front, extending the study of insulating corner-sharing regular tetrahedra systems to normal rare-earth spinel systems is poised to provide more examples of exotic spin dynamics as recently shown [2,53].

ACKNOWLEDGMENTS

We are grateful to P. C. W. Holdsworth and E. Ressouche for discussions. A.Y. acknowledges speakers at the International Workshop on Frustration and Topology in Condensed Matter Physics held at Tainan in February 2014 for clarifying the

nature of excitations in geometrically frustrated compounds. He thanks S. Onoda for his invitation to the workshop. This research project was partially supported by the European Commission under the 6th Framework Programme through the Key Action: Strengthening the European Research Area, Research Infrastructures (Contract No. RII3-CT-2003-505925), and under the 7th Framework Programme through the Research Infrastructures action of the Capacities Programme, NMI3-II Grant No. 283883 (Contract No. CP-CSA_INFRA-2008-1.1.1, No. 226507-NMI3). Part of this work was performed at the Institut Laue Langevin, Grenoble, France, at the muon and neutron sources of the Paul Scherrer Institute, Villigen, Switzerland and at the ISIS pulsed muon facility, Rutherford Appleton Laboratory, Chilton, United Kingdom.

[1] J. S. Gardner, M. J. P. Gingras, and J. E. Greedan, Rev. Mod. Phys. **82**, 53 (2010).
[2] A. Yaouanc, P. Dalmas de Réotier, A. Bertin, C. Marin, E. Lhotel, A. Amato, and C. Baines, Phys. Rev. B **91**, 104427 (2015).
[3] J. Villain, Z. Phys. B **33**, 31 (1979).
[4] M. Hermele, M. P. A. Fisher, and L. Balents, Phys. Rev. B **69**, 064404 (2004).
[5] J. D. M. Champion, M. J. Harris, P. C. W. Holdsworth, A. S. Wills, G. Balakrishnan, S. T. Bramwell, E. Čižmár, T. Fennell, J. S. Gardner, J. Lago, D. F. McMorrow, M. Orendáč, A. Orendáčová, D. M. McK. Paul, R. I. Smith, M. T. F. Telling, and A. Wildes, Phys. Rev. B **68**, 020401 (2003).
[6] I. Mirebeau, A. Apetrei, J. Rodríguez-Carvajal, P. Bonville, A. Forget, D. Colson, V. Glazkov, J. P. Sanchez, O. Isnard, and E. Suard, Phys. Rev. Lett. **94**, 246402 (2005).
[7] A. Yaouanc, P. Dalmas de Réotier, P. Bonville, J. A. Hodges, V. Glazkov, L. Keller, V. Sikolenko, M. Bartkowiak, A. Amato, C. Baines, P. J. C. King, P. C. M. Gubbens, and A. Forget, Phys. Rev. Lett. **110**, 127207 (2013).
[8] J. Lago, T. Lancaster, S. J. Blundell, S. T. Bramwell, F. L. Pratt, M. Shirai, and C. Baines, J. Phys. Condens. Matter **17**, 979 (2005).
[9] P. Dalmas de Réotier, A. Yaouanc, L. Keller, A. Cervellino, B. Roessli, C. Baines, A. Forget, C. Vaju, P. C. M. Gubbens, A. Amato, and P. J. C. King, Phys. Rev. Lett. **96**, 127202 (2006).
[10] A. Yaouanc, P. Dalmas de Réotier, V. Glazkov, C. Marin, P. Bonville, J. A. Hodges, P. C. M. Gubbens, S. Sakarya, and C. Baines, Phys. Rev. Lett. **95**, 047203 (2005).
[11] J. R. Stewart, G. Ehlers, A. S. Wills, S. T. Bramwell, and J. S. Gardner, J. Phys. Condens. Matter **16**, L321 (2004).
[12] A. S. Wills, M. E. Zhitomirsky, B. Canals, J. P. Sanchez, P. Bonville, P. Dalmas de Réotier, and A. Yaouanc, J. Phys. Condens. Matter **18**, L37 (2006).
[13] P. Bonville, J. A. Hodges, E. Bertin, J.-P. Bouchaud, P. Dalmas de Réotier, L.-P. Regnault, H. M. Rønnow, J.-P. Sanchez, S. Sosin, and A. Yaouanc, Hyperfine Interact. **156-157**, 103 (2004).
[14] Y. Chapuis, P. Dalmas de Réotier, C. Marin, A. Yaouanc, A. Forget, A. Amato, and C. Baines, Physica B **404**, 686 (2009).
[15] M. A. Subramanian, G. Aravamudan, and G. V. S. Rao, Prog. Solid State Chem. **15**, 55 (1983).
[16] B. J. Kennedy, B. A. Hunter, and C. J. Howard, J. Solid State Chem. **130**, 58 (1997).
[17] M. E. Brooks-Bartlett, S. T. Banks, L. D. C. Jaubert, A. Harman-Clarke, and P. C. W. Holdsworth, Phys. Rev. X **4**, 011007 (2014).
[18] H. W. J. Blöte, R. F. Wielinga, and W. J. Huiskamp, Physica **43**, 549 (1969).
[19] K. Matsuhira, Y. Hinatsu, K. Tenya, H. Amitsuka, and T. Sakakibara, J. Phys. Soc. Jpn. **71**, 1576 (2002).
[20] P. Dalmas de Réotier, A. Yaouanc, P. C. M. Gubbens, C. T. Kaiser, C. Baines, and P. J. C. King, Phys. Rev. Lett. **91**, 167201 (2003).
[21] P. Dalmas de Réotier, A. Yaouanc, D. E. MacLaughlin, S. Zhao, T. Higo, S. Nakatsuji, Y. Nambu, C. Marin, G. Lapertot, A. Amato, and C. Baines, Phys. Rev. B **85**, 140407 (2012).
[22] V. Bondah-Jagalu and S. T. Bramwell, Can. J. Phys. **79**, 1381 (2001).
[23] A. Bertin, Ph.D. thesis, Université Grenoble Alpes (2015).
[24] J. Rodriguez-Carvajal, Physica B **192**, 55 (1993).
[25] G. Ferey, R. De Pape, M. Leblanc, and J. Pannetier, Rev. Chim. Miner. **23**, 474 (1986).
[26] K. Tomiyasu, K. Matsuhira, K. Iwasa, M. Watahiki, S. Takagi, M. Wakeshima, Y. Hinatsu, M. Yokoyama, K. Ohoyama, and K. Yamada, J. Phys. Soc. Jpn. **81**, 034709 (2012).
[27] J. Yamaura, K. Ohgushi, H. Ohsumi, T. Hasegawa, I. Yamauchi, K. Sugimoto, S. Takeshita, A. Tokuda, M. Takata, M. Udagawa, M. Takigawa, H. Harima, T. Arima, and Z. Hiroi, Phys. Rev. Lett. **108**, 247205 (2012).
[28] S. Tardif, S. Takeshita, H. Ohsumi, J.-i. Yamaura, D. Okuyama, Z. Hiroi, M. Takata, and T.-h. Arima, Phys. Rev. Lett. **114**, 147205 (2015).
[29] H. Sagayama, D. Uematsu, T. Arima, K. Sugimoto, J. J. Ishikawa, E. O'Farrell, and S. Nakatsuji, Phys. Rev. B **87**, 100403 (2013).
[30] A. Heidemann, Z. Phys. **238**, 208 (1970).
[31] G. E. Barberis, D. Davidov, J. P. Donoso, C. Rettori, J. F. Suassuna, and H. D. Dokter, Phys. Rev. B **19**, 5495 (1979).
[32] W. Marshall and S. W. Lovesey, *Theory of Thermal Neutron Scattering* (Clarendon, Oxford, UK, 1971).
[33] A. Yaouanc and P. Dalmas de Réotier, *Muon Spin Rotation, Relaxation, and Resonance: Applications to Condensed Matter* (Oxford University Press, Oxford, UK, 2011).
[34] A. Yaouanc, P. Dalmas de Réotier, Y. Chapuis, C. Marin, G. Lapertot, A. Cervellino, and A. Amato, Phys. Rev. B **77**, 092403 (2008).
[35] F. Bert, P. Mendels, A. Olariu, N. Blanchard, G. Collin, A. Amato, C. Baines, and A. D. Hillier, Phys. Rev. Lett. **97**, 117203 (2006).
[36] P. Dalmas de Réotier, A. Yaouanc, Y. Chapuis, S. H. Curnoe, B. Grenier, E. Ressouche, C. Marin, J. Lago, C. Baines, and S. R. Giblin, Phys. Rev. B **86**, 104424 (2012).
[37] J. Lago, I. Živković, J. O. Piatek, P. Álvarez, D. Hüvonen, F. L. Pratt, M. Díaz, and T. Rojo, Phys. Rev. B **89**, 024421 (2014).
[38] A. Yaouanc and P. Dalmas de Réotier, J. Phys. Condens. Matter **3**, 6195 (1991).
[39] P. Dalmas de Réotier and A. Yaouanc, Phys. Rev. B **52**, 9155 (1995).

[40] P. Dalmas de Réotier, P. C. M. Gubbens, and A. Yaouanc, J. Phys. Condens. Matter **16**, S4687 (2004).
[41] A. G. Redfield, IBM J. Res. Dev. **1**, 19 (1957).
[42] J. S. Gardner, G. Ehlers, N. Rosov, R. W. Erwin, and C. Petrovic, Phys. Rev. B **70**, 180404(R) (2004).
[43] B. G. Ueland, G. C. Lau, R. J. Cava, J. R. O'Brien, and P. Schiffer, Phys. Rev. Lett. **96**, 027216 (2006).
[44] Y. Chapuis, A. Yaouanc, P. Dalmas de Réotier, S. Pouget, P. Fouquet, A. Cervellino, and A. Forget, J. Phys. Condens. Matter **19**, 446206 (2007).
[45] K. C. Rule, G. Ehlers, J. S. Gardner, Y. Qiu, E. Moskvin, K. Kiefer, and S. Gerischer, J. Phys. Condens. Matter **21**, 486005 (2009).
[46] A. Legros, D. H. Ryan, P. Dalmas de Réotier, A. Yaouanc, and C. Marin, J. Appl. Phys. **117**, 17C701 (2015).
[47] A. Maisuradze, P. Dalmas de Réotier, A. Yaouanc, A. Forget, C. Baines, and P. J. C. King, Phys. Rev. B **92**, 094424 (2015).
[48] Y. Nambu, J. S. Gardner, D. E. MacLaughlin, C. Stock, H. Endo, S. Jonas, T. J. Sato, S. Nakatsuji, and C. Broholm, Phys. Rev. Lett. **115**, 127202 (2015).
[49] S. T. Bramwell and M. J. Harris, J. Phys. Condens. Matter **10**, L215 (1998).
[50] Y.-P. Huang, G. Chen, and M. Hermele, Phys. Rev. Lett. **112**, 167203 (2014).
[51] T. Yavors'kii, T. Fennell, M. J. P. Gingras, and S. T. Bramwell, Phys. Rev. Lett. **101**, 037204 (2008).
[52] S. H. Curnoe, Phys. Rev. B **78**, 094418 (2008).
[53] J. Lago, I. Živković, B. Z. Malkin, J. Rodriguez Fernandez, P. Ghigna, P. Dalmas de Réotier, A. Yaouanc, and T. Rojo, Phys. Rev. Lett. **104**, 247203 (2010).